SCIENTIFIC REPORTS
nature research

OPEN

Smart meta-superconductor MgB_2 constructed by the dopant phase of luminescent nanocomposite

Received: 20 December 2018
Accepted: 17 September 2019
Published online: 02 October 2019

Yongbo Li, Honggang Chen, Mingzhong Wang, Longxuan Xu & Xiaopeng Zhao

On the basis of the idea that the injecting energy will improve the conditions for the formation of Cooper pairs, a smart meta-superconductor (SMSC) was prepared by doping luminescent nanocomposite Y_2O_3:Eu^{3+}/Ag in MgB_2. To improve the superconducting transition temperature (T_C) of the MgB_2-based superconductor, two types of Y_2O_3:Eu^{3+}/Ag, which has the strong luminescence characteristic, with different sizes were prepared and marked as m-Y_2O_3:Eu^{3+}/Ag and n-Y_2O_3:Eu^{3+}/Ag. MgB_2 SMSC was prepared through an *ex situ* process. Results show that when the dopant content was fixed at 2.0 wt.%, the T_C of MgB_2 SMSC increased initially then decreased with the increase in the Ag content in the dopant. When the Ag content is 5%, the T_C of MgB_2 SMSC was 37.2–38.0 K, which was similar to that of pure MgB_2. Meanwhile, the T_C of MgB_2 SMSC doped with n-Y_2O_3:Eu^{3+}/Ag increased initially then decreased basically with the increase in the content of n-Y_2O_3:Eu^{3+}/Ag, in which the Ag content is fixed at 5%. The T_C of MgB_2 SMSC doped with 0.5 wt.% n-Y_2O_3:Eu^{3+}/Ag was 37.6–38.4 K, which was 0.4 K higher than that of pure MgB_2. It is thought that the doping luminescent nanocomposite into the superconductor is a new means to improve the T_C of SMSC.

Improving the superconducting critical transition temperature of materials is an important scientific and technical problem in condensed matter physics and materials science. Recently, Fausti *et al.*[1] used mid-infrared femtosecond pulses to transform non-superconducting $La_{1.675}Eu_{0.2}Sr_{0.125}CuO_4$ into a transient 3D superconductor. A similar method was also applied to investigate $YBa_2Cu_3O_{6.5}$[2] and K_3C_{60}[3,4] and good experimental results were achieved. Ye *et al.* have reported the observation of field-induced superconductivity of ZrNCl and MoS_2 by quasi-continuous electrostatic carrier doping achieved by combining liquid and solid gating[5,6]. Drozdov *et al.*[7] reported conventional superconductivity at 203 K under high pressure in a sulfur hydride system. Adu *et al.*[8] increased the T_C of commercial "dirty" MgB_2 by conducting non-substitutional hole-doping of the MgB_2 structure using minute, single-wall carbon nanotube inclusions. In accordance with homogeneous system theory[9], Smolyaninov *et al.*[10–12] stated that a superconducting metamaterial with an effective dielectric response function that is less and approximately equal to zero may exhibit high T_C, and they verified this theory in their subsequent experiments. Recently, Cao *et al.*[13,14] investigated correlated insulator behavior at half-filling in magic-angle graphene superlattices and reported the realization of intrinsic unconventional superconductivity in a 2D superlattice created by stacking two sheets of graphene that are twisted relative to each other at a small angle. Another important method for studying superconductivity is the topological superconductors[15–20], which have attracted great attention in condensed matter physics. However, obtaining a practical superconductor with high T_C remains difficult.

The superconductivity of MgB_2 was discovered in 2001[21]. MgB_2 is a promising material with large-scale applications because of its excellent superconducting properties and simple crystal structure[22–27]. Considering that the T_C of MgB_2 is close to the McMillan temperature limit[28,29], developing an effective experimental method to improve the T_C of MgB_2 is beneficial to its practical application and to the understanding of the superconducting mechanism. Chemical doping is a simple, effective, commonly used method to change the T_C of superconducting materials. However, many experimental results have confirmed that conventional chemical doping decreases the T_C of MgB_2[30–36]. To date, no effective method has been developed to improve the T_C of MgB_2. The use of metamaterial structures to achieve special properties is an important method developed in recent decades[37–41], and it provides a new approach to improve the T_C of superconducting materials.

Smart Materials Laboratory, Department of Applied Physics, Northwestern Polytechnical University, Xi'an, 710072, China. Correspondence and requests for materials should be addressed to X.Z. (email: xpzhao@nwpu.edu.cn)

On the basis of metamaterials, our group investigated the effects of ZnO electroluminescent (EL) material doping on the superconductivity of BSCCO in 2007 and attempted to change the T_C of this superconductor[42]. Meanwhile, it is proposed that the combination of chemical doping and EL excitement, that is, doping EL materials in superconducting materials to form a meta structure, may be an effective method to improve the T_C of superconductors[43]. On the basis of these results, a smart meta-superconductor (SMSC) model for improving the T_C of materials has been proposed recently. In the model, the dopant phase is used to inject energy through its EL under the external field to strengthen the Cooper pairs, thereby achieving the purpose of changing the T_C. Zhang *et al.*[44] prepared MgB_2 doped with Y_2O_3:Eu^{3+} particles through an *in situ* process. Tao *et al.*[45] prepared MgB_2 doped with Y_2O_3:Eu^{3+} nanorods with different EL intensities through an *ex situ* process. Their results indicated that doping EL materials is favorable for the improvement of T_C compared with conventional doping, which always reduces the superconducting transition temperature of the sample. In addition, similar experimental results were obtained by replacing Y_2O_3:Eu^{3+} with Y_3VO_4:Eu^{3+} flakes[46]. Meanwhlie, results also indicated that the T_C can be changed by adjusting the Y_2O_3:Eu^{3+} concentration and EL exciting current[47]. However, there are some problems need to improve in the experiments. Y_2O_3:Eu^{3+} particles or flakes tended to agglomerate during the preparation process and its EL intensity was weak[44–47]. The quality of commercial MgB_2 was poor and its superconducting transition width (ΔT) is 4.6 K[46,47], further experiment and improvement will be needed. Moreover, the dopants would decrease the T_C in the case of double dopants, i.e., simultaneous incorporation of Y_2O_3:Eu^{3+} and nano-Ag into MgB_2[47].

In this paper, a kind of new phase of luminescent nanocomposite Y_2O_3:Eu^{3+}/Ag was prepared by compounding nano Ag into the Y_2O_3:Eu^{3+} matrix directly[48]. The luminescent intensity of Y_2O_3:Eu^{3+}/Ag is three times higher than that of Y_2O_3:Eu^{3+} due to the composite illumination of EL and photoluminescence (PL). Two kinds of nanocomposite illuminator Y_2O_3:Eu^{3+}/Ag with different sizes, namely, micro Y_2O_3:Eu^{3+}/Ag (m-Y_2O_3:Eu^{3+}/Ag) and nano Y_2O_3:Eu^{3+}/Ag flakes (n-Y_2O_3:Eu^{3+}/Ag), are prepared. Meanwhile, a new kind of commercial MgB_2 with a small ΔT of 0.8 K was used. SMSC was prepared by doping Y_2O_3:Eu^{3+}/Ag in MgB_2 through an *ex situ* process[49]. The T_C of the MgB_2-based superconductor is investigated by changing the Ag content in the dopant phase, the sizes of the dopant phase, and the doping concentration. The results indicate that the T_C of MgB_2 doped with 0.5 wt.% n-Y_2O_3:Eu^{3+}/Ag is 37.6–38.4 K, which is 0.4 K higher than that of pure MgB_2, which further confirmed that the SMSC is a new way to improve the critical transition temperatures.

Experiment

Preparation of m-Y_2O_3:Eu^{3+}/Ag and n-Y_2O_3:Eu^{3+}/Ag. Y_2O_3 and Eu_2O_3 were weighed (the atomic ratio of Y and Eu is 0.95:0.05) and dissolved in a beaker with excess concentrated hydrochloric acid and subsequently heated and dried at 70 °C for 2 h to obtain a white precursor. One of the precursor was dissolved in 4 mL of deionized water to form a solution, and ammonium oxalate was added to it dropwise. The solution was subsequently stirred vigorously at 2 °C in a temperature-controlled water bath. A certain amount of $AgNO_3$ was added to the solution after been stirred for 30 min. After another 30 min of stirring, the pH value of the solution was adjusted to 9–10 by adding NaOH. The final solution, designated as solution A, was obtained after another 30 min of stirring. Another precursor was also prepared into solution with 24 mL benzyl alcohol. Octylamine (4 mL) was added dropwise to the solution, which was subsequently stirred for 1 h. Afterward, a certain amount of $AgNO_3$ was added to the solution. After stirring for another hour, another solution was obtained and designated as solution B. Solutions A and B were then transferred to two reaction kettles, respectively. A hydrothermal reaction occurred at 160 °C for 24 h. The products were washed several times with deionized water and absolute ethanol and sintered at 800 °C for 2 h to form Y_2O_3:Eu^{3+}/AgCl. After illumination, the Y_2O_3:Eu^{3+}/AgCl transformed into two kinds of luminescent Y_2O_3:Eu^{3+}/Ag nanocomposite with different sizes and a certain amount of Ag. The two luminescent nanocomposite materials were designated as m-Y_2O_3:Eu^{3+}/Ag and n-Y_2O_3:Eu^{3+}/Ag. Y_2O_3:Eu^{3+}/Ag with different Ag contents was prepared by changing the $AgNO_3$ content. In this paper, Ag contents uniformly refers to the initial nominal atomic ratio of Ag and Y. For example, 5% Ag means that the initial nominal atomic ratio of Ag to Y is 0.05:0.95. Meanwhile, similar method was applied to synthesize Y_2O_3 and Y_2O_3:Sm^{3+}.

Preparation of MgB_2–based SMSC. At a certain ratio, commercial MgB_2 powder (Alfa Aesar) and the luminescent nanocomposite Y_2O_3:Eu^{3+}/Ag were weighed and prepared into an alcohol solution. The two suspensions were sonicated for 20 min, then the dopant was added dropwise to MgB_2. After sonication for more than 20 min, the mixed solution was transferred to a culture dish. Subsequently, the culture dish was placed in a vacuum oven at 60 °C for 4 h to yield a black powder. The powder was pressed into a pellet with a diameter of 11 mm and a thickness of 2 mm and placed in a small tantalum container, which was annealed at 800 °C for 2 h in high-purity argon atmosphere. The MgB_2-based superconductor doped with luminescent nanocomposite materials of different sizes and Ag contents was synthesized to investigative the T_C of SMSC.

Results and Discussion

Figure 1a shows the EL spectra of Y_2O_3, Y_2O_3:Eu^{3+}, m-Y_2O_3:Eu^{3+}/Ag, and n-Y_2O_3:Eu^{3+}/Ag. The Ag content of the luminescent nanocomposite materials was 5.0%. It shows that Y_2O_3 is a non-EL material and becomes a kind of EL material after the addition of a small amount of Eu element. The results also indicate that the EL intensity of the luminescent m-Y_2O_3:Eu^{3+}/Ag nanocomposite and n-Y_2O_3:Eu^{3+}/Ag is remarkably improved primarily due to the composite luminescence of the electroluminescence of Eu^{3+} centric and the surface plasma-enhanced photoluminescence of Ag. Among the four dopants, n-Y_2O_3:Eu^{3+}/Ag had the highest EL intensity. Figure 1b shows the SEM image of m-Y_2O_3:Eu^{3+}/Ag. The surface size and thickness of the m-Y_2O_3:Eu^{3+}/Ag flake are approximately 300 nm and 30 nm, respectively. Figure 1c,d show AFM images of n-Y_2O_3:Eu^{3+}/Ag and Fig. 1d presents a cross section of the AFM image in Fig. 1c. Figure 1e,f show TEM images of n-Y_2O_3:Eu^{3+}/Ag. It can be seen that the

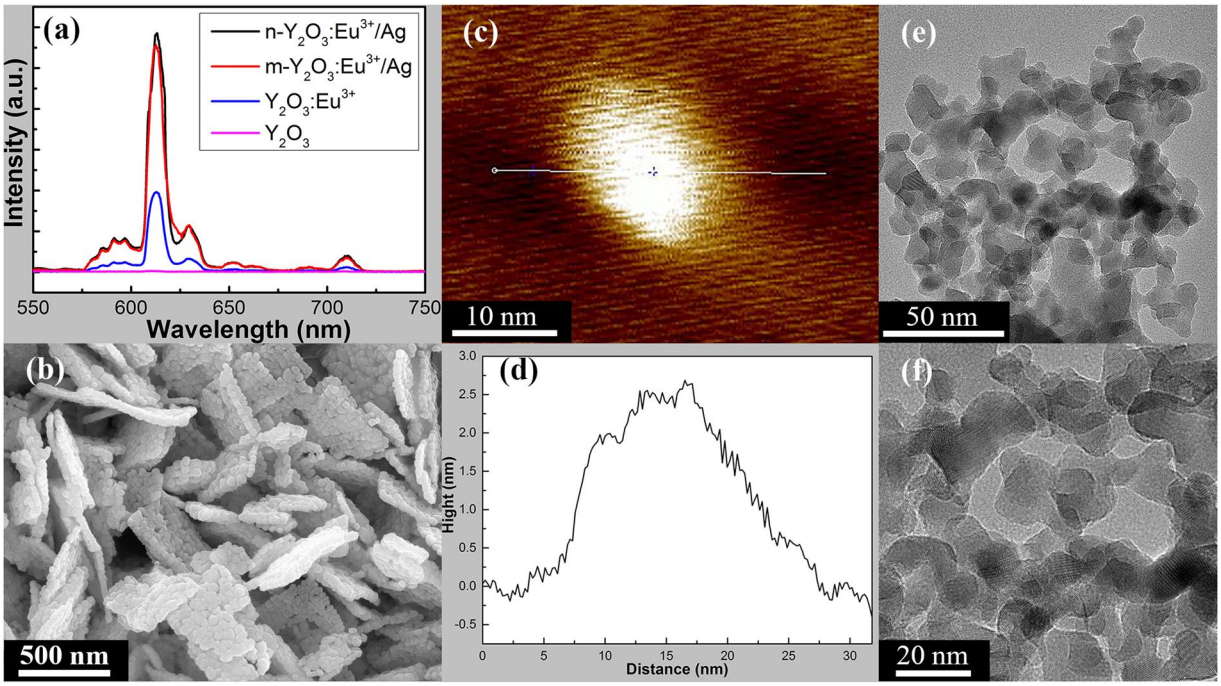

Figure 1. (**a**) EL spectra of Y_2O_3, Y_2O_3:Eu^{3+}, m-Y_2O_3:Eu^{3+}/Ag, and n-Y_2O_3:Eu^{3+}/Ag; (**b**) SEM image of m-Y_2O_3:Eu^{3+}/Ag; (**c**,**d**) AFM images and (**e**,**f**) TEM images of n-Y_2O_3:Eu^{3+}/Ag.

surface size of n-Y_2O_3:Eu^{3+}/Ag was 20 nm, and its thickness was approximately 2.5 nm, which is much smaller than that of m-Y_2O_3:Eu^{3+}/Ag.

Figure 2a shows the SEM image of pure MgB_2. The size of the MgB_2 particle was approximately 0.1–1 μm. The T_C of the samples was determined based on the *R*–*T* curve, which was measured using a four-probe method in a liquid helium cryogenic system developed by the Advanced Research Systems Company. Figure 2b shows the normalized *R*–*T* curve of pure MgB_2 and indicates that the onset temperature ($T_{on\,c}$) and offset temperature ($T_{off\,c}$)[50,51] of pure MgB_2 were 38.0 and 37.2 K, respectively. The ΔT of pure MgB_2 was 0.8 K. Figure 2c shows the XRD spectra of pure MgB_2 and partially doped samples, in which the standard card of MgB_2 (PDF#38-1369) is demonstrated using black vertical lines. The results showed that the XRD spectrum of pure MgB_2 (black curve) matched the standard card of MgB_2 well, except for the inevitable small amount of the MgO phase[52–55]. The red and blue curves represent the XRD spectra of MgB_2 doped with 2.0 wt.% m-Y_2O_3:Eu^{3+}/Ag and 2.0 wt.% n-Y_2O_3:Eu^{3+}/Ag, respectively. The Ag content was 5.0%. The main phase of the doped samples was MgB_2. Moreover, apart from a small amount of the MgO phase, the Y_2O_3 phase was also found in the XRD spectra of the doped samples. The XRD spectra of the other doped samples were similar.

Figure 3 shows the normalized *R*–*T* curves of MgB_2 doped with m-Y_2O_3:Eu^{3+}/Ag with different Ag contents. On the basis of the results of our previous study[45,46], the content of m-Y_2O_3:Eu^{3+}/Ag in the four samples was fixed at 2.0 wt.%. The Ag contents of m-Y_2O_3:Eu^{3+}/Ag in the four samples were 1.0%, 4.0%, 5.0%, and 8.0%, as shown in the figure, and their T_C values were 34.8–35.6, 36.0–36.8, 37.2–38.0, and 34.8–35.6 K, respectively. The T_C of the doped samples initially increased then decreased with the increase in Ag content. Meanwhile, the corresponding doped sample had the highest T_C when the concentration of m-Y_2O_3:Eu^{3+}/Ag was fixed at 2.0 wt.% and the Ag content was 5.0%, which is equal to that of pure MgB_2. The experimental results are similar to those of our previous studies, that is, doping EL materials may improve T_C in several cases compared with conventional doping, which always reduces the T_C of the sample. As a dopant, m-Y_2O_3:Eu^{3+}/Ag exerts an impurity effect that decreases T_C. Meanwhile, as an EL material, m-Y_2O_3:Eu^{3+}/Ag exerts an EL exciting effect that increases T_C[45,46]. An obvious competitive relationship exists between the impurity effect and the EL exciting effect. The final T_C of the samples increased when the EL exciting effect was fully utilized and the impurity effect was minimized.

Figure 4 shows the normalized *R*–*T* curves of MgB_2 doped with 0.1–2.0 wt.% n-Y_2O_3:Eu^{3+}/Ag. Ag concentration was fixed at 5.0%. It can be seen that T_C of MgB_2 doped with n-Y_2O_3:Eu^{3+}/Ag initially decreased, increased, then decreased again with the increase in doping concentration. A too low or too high doping concentration reduces T_C, which is similar to the finding of our previous study. When the doping concentration was in a low range, T_C decreased with the increase in doping concentration due to the dominance of the impurity effect of the dopant, which is similar to the results of conventional doping. The EL exciting effect of the dopant dominated with the further increase in doping concentration, resulting in the increase in T_C. The samples doped with 0.5 wt.% n-Y_2O_3:Eu^{3+}/Ag had the highest T_C of 37.6–38.4 K, which is 0.4 K higher than that of pure MgB_2. However, the impurity effect of the dopant dominated when the doping concentration increased to a high range, which led to a low T_C. These results indicate that doping luminescent nanocomposite materials effectively adjusts and improves T_C at an appropriate doping concentration.

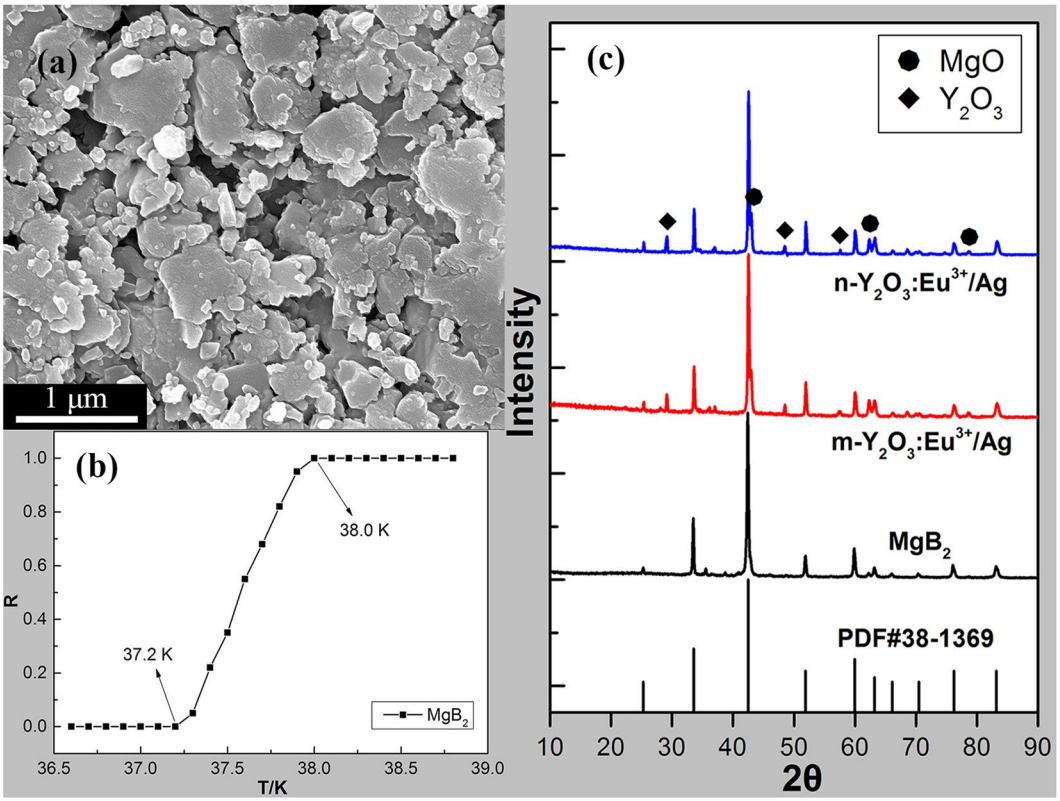

Figure 2. (**a**) SEM image and (**b**) normalized temperature-dependent resistivity (*R*–*T*) curve of pure MgB_2; (**c**) XRD spectra of pure MgB_2 and MgB_2 doped with 2.0 wt.% m-Y_2O_3:Eu^{3+}/Ag and 2.0 wt.% n-Y_2O_3:Eu^{3+}/Ag.

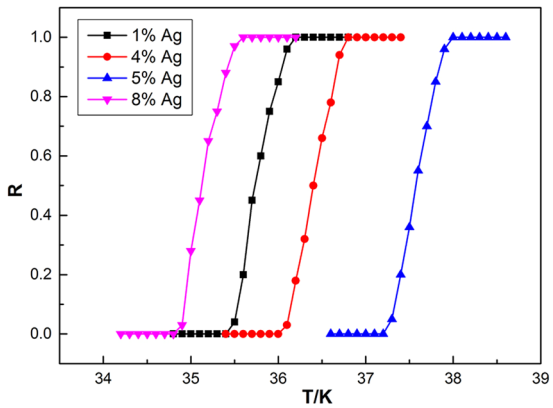

Figure 3. Normalized *R*–*T* curves of MgB_2 doped with 2.0 wt.% m-Y_2O_3:Eu^{3+}/Ag with different Ag contents.

MgB_2 doped with non-EL materials Y_2O_3 and Y_2O_3:Sm^{3+} were synthesized to prove the conclusions above. Figure 5 shows the normalized *R*–*T* curves of MgB_2 doped with Y_2O_3, Y_2O_3:Sm^{3+}, Y_2O_3:Eu^{3+}, and n-Y_2O_3:Eu^{3+}/Ag. The doping concentration was fixed at 0.6 wt.%, and the Ag content in n-Y_2O_3:Eu^{3+}/Ag was 5.0%. Results indicated that T_C of MgB_2 doped with non-EL materials Y_2O_3 or Y_2O_3:Sm^{3+} was much lower than that of pure MgB_2, which is different from MgB_2 doped with EL materials at the same concentration. MgB_2 doped with Y_2O_3:Eu^{3+} increased to 36.6–37.4 K due to the EL exciting effect. Meanwhile, MgB_2 doped with the luminescent n-Y_2O_3:Eu^{3+}/Ag nanocomposite further increased to 37.0–37.8 K. The results show that doping EL materials facilitates an increase in T_C in several cases compared with conventional doping, which always reduces the T_C of the sample. Meanwhile, luminescent Y_2O_3:Eu^{3+}/Ag nanocomposite materials increase the T_C of MgB_2 due to the strong EL intensity.

The results in Fig. 4 show that the optimum concentration of n-Y_2O_3:Eu^{3+}/Ag is 0.5 wt.%, which is lower than the value in our previous study[44–46] due to the small size of n-Y_2O_3:Eu^{3+}/Ag. The disadvantages caused by the impurity effect can be reduced if luminescent nanocomposite materials have a small size and are relatively evenly

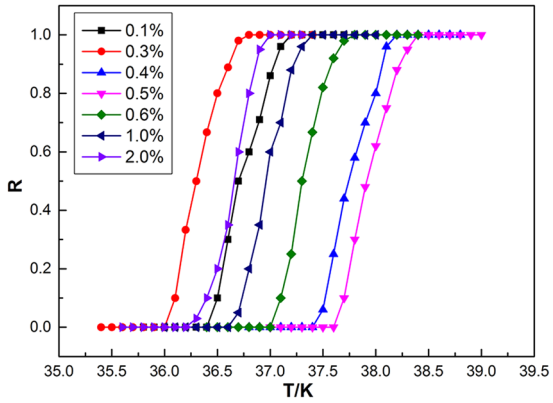

Figure 4. Normalized R–T curves of MgB_2 doped with n-Y_2O_3:Eu^{3+}/Ag.

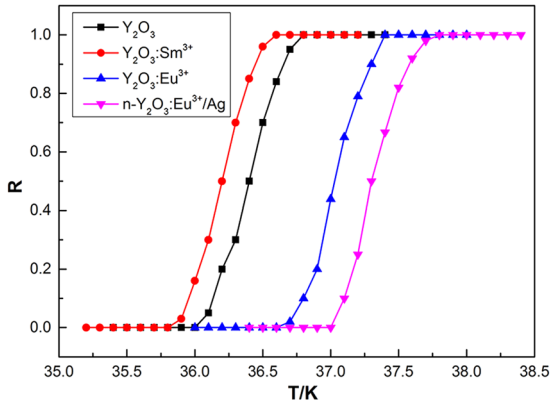

Figure 5. Normalized R–T curves of MgB_2 doped with Y_2O_3, Y_2O_3:Sm^{3+}, Y_2O_3:Eu^{3+}, and n-Y_2O_3:Eu^{3+}/Ag.

distributed in the sample. Moreover, the ΔT of commercial MgB_2 in our previous study[46] was too large to accurately determine the influence of the dopant phase on T_C. In the current study, a new kind of commercial MgB_2 with a small ΔT of 0.8 K was used, and we obtained a similar conclusion, which further proves the effectiveness of this method.

Conclusions

In this paper, two types of luminescent nanocomposite Y_2O_3:Eu^{3+}/Ag with different sizes were prepared and marked as m-Y_2O_3:Eu^{3+}/Ag and n-Y_2O_3:Eu^{3+}/Ag. SEM and AFM images indicated that the surface size and thickness of m-Y_2O_3:Eu^{3+}/Ag are approximately 300 nm and 30 nm, which are 20 nm and 2.5 nm for n-Y_2O_3:Eu^{3+}/Ag. The EL spectra showed that the luminescent intensity of Y_2O_3:Eu^{3+}/Ag is three times higher than that of Y_2O_3:Eu^{3+}. MgB_2 of SMSC was prepared through an *ex situ* process to improve the T_C of the MgB_2-based superconductor on the basis of the idea that the injecting energy will improve the conditions for the formation of Cooper pairs. The T_C of MgB_2 SMSC was determined based on the measured R–T curve by using the four-probe method in a liquid helium cryogenic system. Results show that the T_C of MgB_2 SMSC initially increased then decreased with the increase in the Ag content when m-Y_2O_3:Eu^{3+}/Ag content was fixed at 2.0 wt.%. When the Ag content was 5.0%, the T_C of MgB_2 SMSC doped with 2.0 wt.% m-Y_2O_3:Eu^{3+}/Ag was 37.2–38.0 K, which was equal to that of pure MgB_2. Meanwhile, the T_C of MgB_2 SMSC doped with n-Y_2O_3:Eu^{3+}/Ag increased initially then decreased basically with the increase in the content of n-Y_2O_3:Eu^{3+}/Ag, in which the Ag content is fixed at 5%. The T_C of MgB_2 SMSC doped with 0.5 wt.% n-Y_2O_3:Eu^{3+}/Ag was 37.6–38.4 K, which was 0.4 K higher than that of pure MgB_2. It is thought that the doping luminescent nanocomposite into the superconductor is a new means to improve the T_C of SMSC. However, the increase in the T_C remains insufficient. In future work, new dopant phases with improved characteristics will be prepared to increase the T_C of MgB_2. Meanwhile, we will attempt to apply this method to other superconductors.

References

1. Fausti, D. *et al.* Light-Induced Superconductivity in a Stripe-Ordered Cuprate. *Science* **331**, 189–191 (2011).
2. Hu, W. *et al.* Optically enhanced coherent transport in $YBa_2Cu_3O_{6.5}$ by ultrafast redistribution of interlayer coupling. *Nat. Mater.* **13**, 705–711 (2014).
3. Mitrano, M. *et al.* Possible light-induced superconductivity in K_3C_{60} at high temperature. *Nature* **530**, 461–464 (2016).
4. Cantaluppi, A. *et al.* Pressure tuning of light-induced superconductivity in K_3C_{60}. *Nat. Phys.* **14**, 837–841 (2018).

5. Ye, J. T. *et al*. Liquid-gated interface superconductivity on an atomically flat film. *Nat. Mater.* **9**, 125–128 (2010).
6. Ye, J. T. *et al*. Superconducting Dome in a Gate-Tuned Band Insulator. *Science* **338**, 1193–1196 (2012).
7. Drozdov, A. P., Eremets, M. I., Troyan, I. A., Ksenofontov, V. & Shylin, S. I. Conventional superconductivity at 203 kelvin at high pressures in the sulfur hydride system. *Nature* **525**, 73–76 (2015).
8. Ma, D. H. *et al*. Enhancing the superconducting temperature of MgB_2 by SWCNT dilution. *Physica C* **497**, 43–48 (2014).
9. Kirzhnits, D. A., Maksimov, E. G. & Khomskii, D. I. The description of superconductivity in terms of dielectric response function. *J. Low Temp. Phys.* **10**, 79–93 (1973).
10. Smolyaninova, V. N. *et al*. Experimental demonstration of superconducting critical temperature increase in electromagnetic metamaterials. *Sci. Rep.* **4**, 7321 (2014).
11. Smolyaninova, V. N. *et al*. Using metamaterial nanoengineering to triple the superconducting critical temperature of bulk aluminum. *Sci. Rep.* **5**, 15777 (2015).
12. Smolyaninov, I. I. & Smolyaninova, V. N. Theoretical modeling of critical temperature increase in metamaterial superconductors. *Phys. Rev. B* **93**, 184510 (2016).
13. Cao, Y. *et al*. Correlated insulator behaviour at half-filling in magic-angle graphene superlattices. *Nature* **556**, 80–84 (2018).
14. Cao, Y. *et al*. Unconventional superconductivity in magic-angle graphene superlattices. *Nature* **556**, 43–50 (2018).
15. Qi, X. L. & Zhang, S. C. Topological insulators and superconductors. *Rev. Mod. Phys.* **83**, 1057–1110 (2011).
16. Wang, Z., Qi, X. L. & Zhang, S. C. Topological field theory and thermal responses of interacting topological superconductors. *Phys. Rev. B* **84**, 014527 (2011).
17. Leijnse, M. & Flensberg, K. Introduction to topological superconductivity and Majorana fermions. *Semicond. Sci. Technol.* **27**, 124003 (2012).
18. Schnyder, A. P. & Brydon, P. M. Topological surface states in nodal superconductors. *J. Phys.: Condens. Matter* **27**, 243201 (2015).
19. Sato, M. & Ando, Y. Topological superconductors: a review. *Rep. Prog. Phys.* **80**, 076501 (2017).
20. Fatemi, V. *et al*. Electrically tunable low-density superconductivity in a monolayer topological insulator. *Science*, https://doi.org/10.1126/science.aar4642 (2018).
21. Nagamatsu, J., Nakagawa, N., Muranaka, T., Zenitani, Y. & Akimitsu, J. Superconductivity at 39 K in magnesium diboride. *Nature* **410**, 63–64 (2001).
22. Buzea, C. & Yamashita, T. Review of the superconducting properties of MgB_2. *Supercond. Sci. Technol.* **14**, R115–R146 (2001).
23. Eisterer, M. Magnetic properties and critical currents of MgB_2. *Supercond. Sci. Technol.* **20**, R47–R73 (2007).
24. Vinod, K., Varghese, N. & Syamaprasad, U. Superconductivity of MgB_2 in the BCS framework with emphasis on extrinsic effects on critical temperature. *Supercond. Sci. Technol.* **20**, R31–R45 (2007).
25. Xi, X. X. Two-band superconductor magnesium diboride. *Rep. Prog. Phys.* **71**, 116501 (2008).
26. Ma, Z. Q., Liu, Y. C. & Cai, Q. The synthesis of lamellar nano MgB_2 grains with nanoimpurities, flux pinning centers and their significantly improved critical current density. *Nanoscale* **4**, 2060–2065 (2012).
27. Prikhna, T. A. *et al*. Nanostructural inhomogeneities acting as pinning centers in bulk MgB_2 with low and enhanced grain connectivity. *Supercond. Sci. Technol.* **27**, 044013 (2014).
28. Bardeen, J., Cooper, L. N. & Schrieffer, J. R. Theory of Superconductivity. *Phys. Rev.* **108**, 1175–1204 (1957).
29. McMillan, W. L. Transition Temperature of Strong-Coupled Superconductors. *Phys. Rev.* **167**, 331–344 (1968).
30. Slusky, J. S. *et al*. Loss of superconductivity with the addition of Al to MgB_2 and a structural transition in $Mg_{1-x}Al_xB_2$. *Nature* **410**, 343–345 (2001).
31. Zhao, Y. G. *et al*. Effect of Li doping on structure and superconducting transition temperature of $Mg_{1-x}Li_xB_2$. *Physica C* **361**, 91–94 (2001).
32. Luo, H., Li, C. M., Luo, H. M. & Ding, S. Y. Study of Al doping effect on superconductivity of $Mg_{1-x}Al_xB_2$. *J. Appl. Phys.* **91**, 7122–7124 (2002).
33. Cava, R. J., Zandbergen, H. W. & Inumaru, K. The substitutional chemistry of MgB_2. *Physica C* **385**, 8–15 (2003).
34. Kazakov, S. M. *et al*. Carbon substitution in MgB_2 single crystals: Structural and superconducting properties. *Phys. Rev. B* **71**, 024533 (2005).
35. Bianconi, A. *et al*. Controlling the Critical Temperature in $Mg_{1-x}Al_xB_2$. *J. Supercond. Nov. Magn.* **20**, 495–501 (2007).
36. Monni, M. *et al*. Role of charge doping and lattice distortions in codoped $Mg_{1-x}(AlLi)_xB_2$ compounds. *Physica C* **460–462**, 598–599 (2007).
37. Liu, H., Zhao, X. P., Yang, Y., Li, Q. W. & Lv, J. Fabrication of Infrared Left-Handed Metamaterials via Double Template-Assisted Electrochemical Deposition. *Adv. Mater.* **20**, 2050–2054 (2008).
38. Qiao, Y. P., Zhao, X. P. & Su, Y. Y. Dielectric metamaterial particles with enhanced efficiency of mechanical/electrical energy transformation. *J. Mater. Chem.* **21**, 394–399 (2011).
39. Kurter, C. *et al*. Switching nonlinearity in a superconductor-enhanced metamaterial. *Appl. Phys. Lett.* **100**, 121906 (2012).
40. Zhao, X. P. Bottom-up fabrication methods of optical metamaterials. *J. Mater. Chem.* **22**, 9439–9449 (2012).
41. Ma, X. *et al*. Meta-Chirality: Fundamentals, Construction and Applications. *Nanomaterials* **7**, 116 (2017).
42. Jiang, W. T., Xu, Z. L., Chen, Z. & Zhao, X. P. Introduce uniformly distributed ZnO nano-defects into BSCCO superconductors by nano-composite method. *J. Funct. Mater* 38, 157–160, in Chinese, available at, http://www.cnki.com.cn/Article/CJFDTOTAL-GNCL200701046.htm (2007).
43. Xu, S. H., Zhou, Y. W. & Zhao, X. P. Research and Development of Inorganic Powder EL Materials. *Mater. Rev*. **21**, 162–166, in Chinese, available at, http://www.cnki.com.cn/Article/CJFDTotal-CLDB2007S3048.htm (2007).
44. Zhang, Z. W., Tao, S., Chen, G. W. & Zhao, X. P. Improving the Critical Temperature of MgB_2 Superconducting Metamaterials Induced by Electroluminescence. *J. Supercond. Nov. Magn.* **29**, 1159–1162 (2016).
45. Tao, S., Li, Y. B., Chen, G. W. & Zhao, X. P. Critical Temperature of Smart Meta-superconducting MgB_2. *J. Supercond. Nov. Magn.* **30**, 1405–1411 (2017).
46. Li, Y. B., Chen, H. G., Qi, W. C., Chen, G. W. & Zhao, X. P. Inhomogeneous Phase Effect of Smart Meta-Superconducting MgB_2. *J. Low Temp. Phys.* **191**, 217–227 (2018).
47. Chen, H. G., Li, Y. B., Chen, G. W., Xu, L. X. & Zhao, X. P. The Effect of Inhomogeneous Phase on the Critical Temperature of Smart Meta-superconductor MgB_2. *J. Supercond. Nov. Magn.* **31**, 3175–3182 (2018).
48. Wang, M. Z., Xu, L. X., Chen, G. W. & Zhao, X. P. Topological luminophor Y2O3:Eu^{3+} + Ag with high electroluminescence performance. *ACS Appl. Mater. Interfaces* **11**, 2328–2335 (2019).
49. Zhao, X. P., Li, Y. B., Chen, H. G. & Chen, G. W. MgB_2-based superconductor constructed by inhomogeneous phase of topological illuminator and its preparation method. *Chinese Patent* 201810462942.X.
50. Kušević, I. *et al*. Flux pinning and critical currents in polycrystalline MgB_2. *Solid State Commun.* **122**, 347–350 (2002).
51. Bhadauria, P. P. S., Gupta, A., Kishan, H. & Narlikar, A. V. Connectivity and critical current density of *in-situ* processed MgB_2 superconductors: Effect of excess Mg and non-carbon based additives. *J. Appl. Phys.* **115**, 183905 (2014).
52. Eyidi, D. *et al*. Phase analysis of superconducting polycrystalline MgB_2. *Micron* **34**, 85–96 (2003).
53. Shi, Q. Z., Liu, Y. C., Gao, Z. M. & Zhao, Q. Formation of MgO whiskers on the surface of bulk MgB_2 superconductors during *in situ* sintering. *J. Mater. Sci.* **43**, 1438–1443 (2007).
54. Ma, Z. Q., Liu, Y. C., Shi, Q. Z., Zhao, Q. & Gao, Z. M. The improved superconductive properties of MgB_2 bulks with minor Cu addition through reducing the MgO impurity. *Physica C* **468**, 2250–2253 (2008).
55. Singh, D. K., Tiwari, B., Jha, R., Kishan, H. & Awana, V. P. S. Role of MgO impurity on the superconducting properties of MgB_2. *Physica C* **505**, 104–108 (2014).

Acknowledgements
This work was supported by the National Natural Science Foundation of China for Distinguished Young Scholar under Grant No. 50025207.

Author Contributions
X.Z. conceived and led the project; Y.L., H.C. and X.Z. designed the experiments; Y.L., H.C., M.W. and L.X. performed the experiments and characterized the samples; all authors discussed and analyzed the results; Y.L. wrote the paper with input from all co-authors; X.Z. and Y.L. discussed the results and revised the manuscript.

Additional Information
Competing Interests: The authors declare no competing interests.

Publisher's note Springer Nature remains neutral with regard to jurisdictional claims in published maps and institutional affiliations.